**Scientia*et*Fides** 12(2)/2024 ISSN 2300-7648 (print) / ISSN 2353-5636 (online)

Received: May 17, 2024. Accepted: June 6, 2024 DOI: http://dx.doi.org/10.12775/SetF.2024.020

# New Insights on the Turin Shroud's Body Image: Face Image at Different Wavelengths and its Double Superficiality

**LIBERATO DE CARO**
Consiglio Nazionale delle Ricerche (IC-CNR)
liberato.decaro@cnr.it
ORCID: 0000-0002-7927-6178

**GIULIO FANTI**
Università di Padova, Padova
giulio.fanti@unipd.it
ORCID: 0000-0003-4584-4488

**Abstract.** Various images of the face of the Turin Shroud Man, acquired at different wavelengths, from the near infrared region to the ultraviolet, have been studied and compared. A correlation as a function of the wavelength, between the penetration depth in the fabric of the incident light and the anatomic details visible on the images, is discussed based on the physical properties of linen threads and light. In addition, the backside of the Turin Shroud, in correspondence of the region of the face, has been examined, evidencing the possible presence of a second superficial image impressed on the backside. Notwithstanding the high level of scientific knowledge today reached, there is no known physical/chemical process which allows to explain all the properties of the Turin Shroud's body image. According to our scientific knowledge, the corpse of a dead man cannot produce an energy capable to imprint on a linen cloth an image with all the microscopical and macroscopical properties discovered by analyzing the body image of the Turin Shroud, which has not yet been reproduced in any laboratory in the world. According to faith the corpse of a living Man can do it, during the resurrection, assuming a different state of matter. With this respect, the Turin Shroud can be considered as a two-thousand-old relic wit-

nessing to the humanity, just in the age of science, the reasonableness of the faith in the resurrection.

**Keywords:** Turin Shroud, light attenuation length, linen fabric, body image, resurrection, Jesus of Nazareth.

## Introduction

The Turin Shroud (TS) is the most studied archaeological and religious object in the world. Indeed, the TS boasts not only dozens of publications in specialized scientific journals (Jumper et al. 1984; Schwalbe and Rogers 1982), but also hundreds of books in dozens of different languages (Adler 2014; Antonacci 2016; Barbet 2014; Fanti and Malfi 2015a; De Caro and Matricciani 2024; De Caro 2020; De Caro 2024) to divulgate the main results of the research, together with articles and notes that appear almost daily in newspapers and in the web.

The TS is an ancient linen cloth, 4.4 m long and 1.1 m wide, which enveloped the corpse of a tortured man, scourged, crowned with thorns, crucified and pierced by a spear in the chest. Many researchers are convinced that the TS is the sepulchral cloth of Jesus Christ. The body image, impressed on it, has been the subject of intense studies, especially during the twentieth century but, even today, it is not technically reproducible and cannot even be explained in a scientific way (Jumper et al. 1984; Schwalbe and Rogers 1982; Fanti 2011; 2023). Among the many hypotheses proposed, that of a burst of energy coming from inside the body (Fanti 2011; Jackson 2017) could explain the presence of body image in correspondence of anatomical areas, like that one between the cheek and the nose, that were not in contact with the human body. Moreover, this hypothesis could also explain the absence of lateral deformations of the face's image, that would be unavoidable if the body image had been made by direct contact with the corpse, the so-called Agamemnon Mask's deformation.

On the Shroud, several signs are visible, not easily comprehensible at first glance: the double mirror image –frontal and dorsal– of a man, the bloodstains corresponding to his wounds when he was wrapped,

the stains caused by water, the traces and the holes caused by the fire of Chambéry of 1532 and other minor signs.

In 1988 the TS was radiocarbon dated by three famous laboratories (Damon et al. 1989), and it turned out to be attributed to the year 1325 AD, with uncertainty of ±65 years. This result has been widely criticized[10-12] (Rogers 2005; Riani et al. 2013; Fanti et al. 2015b; Casabianca et al. 2019) both for procedural and statistical deficiencies. Other independent methods indicates that the TS could also be of the first century of the Christian era (Fanti et al. 2015b; Fanti 2018; De Caro et al. 2019a; 2022a; 2022b).

Many historians (Antonacci 2016: Wilson 2011) identify the TS with the Mandylion, kept in Edessa, the current Salinurfa in Turkey, in the early centuries. Other hypotheses have been also proposed, as the Christ of Beirut (De Caro et al. 2022b). In any case, the TS reached Constantinople, where remained until the siege and sack of the city in 1204. The TS reappeared in Lirey in 1353, and it was subsequently kept in Chambery since 1502, where a fire damaged it in 1532. In 1578, it was brought to Turin where it is still kept (De Caro et al. 2022b).

During the STuRP (Shroud of Turin Research Project) campaign in 1978 (Jumper et al. 1984; Schwalbe and Rogers 1982), W. Miller, with D. Devan (1982) made photographs of the TS body image's face at different wavelengths in the visible range.[1] G. B. Judica Cordiglia in 1969, during his acquisitions, illuminated the cloth with ultraviolet (UV) emitted by two mercury vapor lamps (Cordiglia 1976; 1988). Judica Cordiglia made photographs of the face not only in the UV wavelength range, but also with near infrared (NIR) radiation. G. Durante in 2002 (Ghiberti, 2002) photographed the backside of the Shroud with visible light.

Up to now there are no published studies on the changes that can be visible on the face of the TS Man acquired at different wavelengths. Indeed, no study has compared all the acquired images together. For this reason, in the present paper, we will study how the visibility of the different anatomical details of the TS Man's face depends on the attenua-

[1] The images taken by V. Miller with red, blue and green light, used in this work, have been bought by the second author from Giorgio Bracaglia C/O Holy Shroud Guild PPF (USA). G. Bracaglia scanned the original 35 mm negative slides of V. Miller, labeled as "natural color", by using an Imacon Flextight Precision II scanner.

tion length of the radiation used to illuminate the cloth, to obtain further indications about the depth of the body image coloration. This finding will be useful both to study a characteristic of the TS image, not enough clarified, i.e., whether a feeble anatomical feature of the face is visible on the backside of the TS (Fanti and Maggiolo 2004; Balossino 2003; Fanti 2003; Fanti and Maggiolo 2014; Di Lazzaro et al. 2013), and to add further quantitative information about the physical properties of the TS image, which has not yet reproduced in any laboratory in the world, notwithstanding the technology and scientific knowledge today available. With this respect, the TS seems to become more and more, precisely in the age of science, a convincing argument on the reasonableness of the faith in the resurrection of Jesus of Nazareth (Jackson 1998, Moran & Fanti 2002).

## 1. Physical and chemical properties of the TS body image

In this section, we briefly summarize the main chemical/physical properties of the TS body image and the main hypotheses proposed by scholars to explain, at least partially, some of these properties, although no hypothesis explains all the peculiar characteristics of the TS body image (Jumper et al. 1984; Schwalbe and Rogers 1982; Fanti, 2011; 2023).

The body image is due to chemical reactions of the polysaccharides composing the linen fibers: oxidation, dehydration and conjugation. For this reason, it is not a painted image. The body image has the tones of light and dark reversed, which gives it many features of a photographic negative. The luminance distribution of both front and back body images can be correlated to the clearances between the body surface and the covering cloth thus producing a 3D effect. The body image is present also in body-sheet noncontact zones, for example, between nose and the cheek. Ultraviolet radiation produces no fluorescence of the body image. The body image has a resolution of 4.9 mm ±0.5 mm, but no well-defined contours. So, while details such as nose and lips are visible, the body image seems to disappear when looking at it from a distance less than about 1 m. The rigor mortis of the dead body seems to be detectable by the non-flattened image of the gluteal area, because a flaccid body with relaxed

muscles, placed supine on a slab, would have given rise to a much larger contact area in correspondence with this anatomic part on the burial cloth (Bevilacqua et al. 2018), although contraction of gluteal muscles of a living person, returned from death to life and moving within the TS, should be also considered (Hontanilla 2022). Putrefaction signs are absent on the body image. The colored image fibers are concentrated only on the uppermost portions, are absent on the threads crossing in the cloth's weave, are adjacent to non-image fibers. Striations are evident on the threads. In the crevices where threads cross each other there is a concentration of color intensity. The color is uniform around the cylindrical fibers' surface, whereas intensity variations appear along the fiber's axis. While the cellulose of the lumen is colorless, the color is evident on the 200 nm thin layer that can be recognized as the primary cell wall of the fibers. The colored fibers are confined in a very thin thickness up to a maximum depth from the surface of about three microfibers. No cementation between fibers or signs of capillary flow appears in the image areas while it can be detected in the bloodstains' areas. The red stains are predominantly composed of blood and frequently surrounded by serum haloes. As no image appears under the bloodstains, we must suppose that these formed before the body image. Some blood dripped from the corpse to the fabric in correspondence of the elbows where it traced rivulets outside the body image.

Some scholars assert that the body image could have been produced by an artist who could have painted it or produced it from a bas relief or using more elaborate techniques such as using acids. However, the properties at the microscopic level (e.g. the maximum depth of the colored microfibers) excludes both the bas-relief technique and the use of acids. Other scholars proposed a body–cloth direct contact mechanism as an explanation of the image formation, in a way similar to the leaves imprint in old herbaria. However, this hypothesis fails to consider that the body image exists even where the cloth would not have been in contact with the body. Other studies proposed a diffusion mechanism (vaporigraph hypothesis) to explain the formation of the body image, related to decomposition gases (ammonia vapor) developed between the corpse and the linen sheet which could have reacted with the cloth, triggering a chemi-

cal reaction of the linen. But the body image is characterized by an almost vertical projection on the cloth, a property which cannot be explained by vapour/gas diffusion which does not happen in a well-defined angular direction. Also, a mechanism based on the Maillard reaction has been proposed, supposing the presence of amines produced by the decomposition of the corpse, but this goes against the evidence that the corpse was wrapped with antiputride substances for no more than forty hours, thus not allowing the formation of putrefaction gases. Therefore, the Maillard reaction could only be thought if an energy, perhaps of electric type, acted in conjunction with the decomposition of urea exudate from the corpse (Fanti 2023, Fanti and Siefker 2024).

Even soft X-rays could decompose urea in ammonia, a chemical compound which can accelerate the natural aging of the polysaccharides composing the body-image linen fibers, increasing locally the yellowing of linen fibers, as seen in the TS body image (De Caro 2020; De Caro 2024). Indeed, given that the body image is visible on the linen fabric where there was certainly no contact between the body and the cloth, many scholars have supposed that it was a radiation, i.e. a phenomenon acting at a distance, to form the body image. This hypothesis appears to be congruent with many body image characteristics, but a corpse of a dead man cannot give off radiant energy in the wavelength range – e.g. ultraviolets, soft X-rays – needed to activate the processes of oxidation, dehydration and conjugation of the polysaccharides composing the body-image linen fibers. A particular radiation hypothesis is related with the Corona Discharge (CD) produced by an intense electric field. But even in this case a corpse of a dead man cannot generate CD.

Summarizing, notwithstanding our scientific knowledges, no experimental attempt was successful to obtain a body image with all the properties evidenced by the studied on the TS. Moreover, the most promising techniques require sources of energy which cannot be emitted by a corpse of a dead man. Therefore, also for the science of the XXI century of Christian era, the formation of the TS body image remains still an unexplained phenomenon. In the next section we will further analyze the body image, in the region of the face, to search further information about its physical properties.

## 2. Logarithmic display of the Turin Shroud image

As already underlined, the positive TS image $I(x, y)$ shows the dark-light contrast inverted as a function of the pixel coordinates $x$ and $y$. Figure 1a shows the original image of the TS face's region, extracted by a 2002 photograph taken by G. C. Durante. By converting the positive TS image in gray levels, the intensity $I(x, y)$ is obtained, as a function of the coordinates $(x, y)$. This function fully describes the image plane. As accidentally found after developing the glass plate of the photograph just taken by S. Pia in 1898, the display of the complementary image $1 - I(x, y)$ shows the correct black and white contrast of a human face (Figure 1b).

Moreover, it is well known that both $I(x, y)$ and $1 - I(x, y)$ contain tridimensional information, some way related to the distance $z(x, y)$ between the different anatomical parts of the corpse and the wrapping sheet. In fact, luminance levels of the body image turn out to be proportional to the hypothetical distance of the body-wrapping burial cloth. In fact, the chemical/physical mechanism of image formation embedded tridimen-

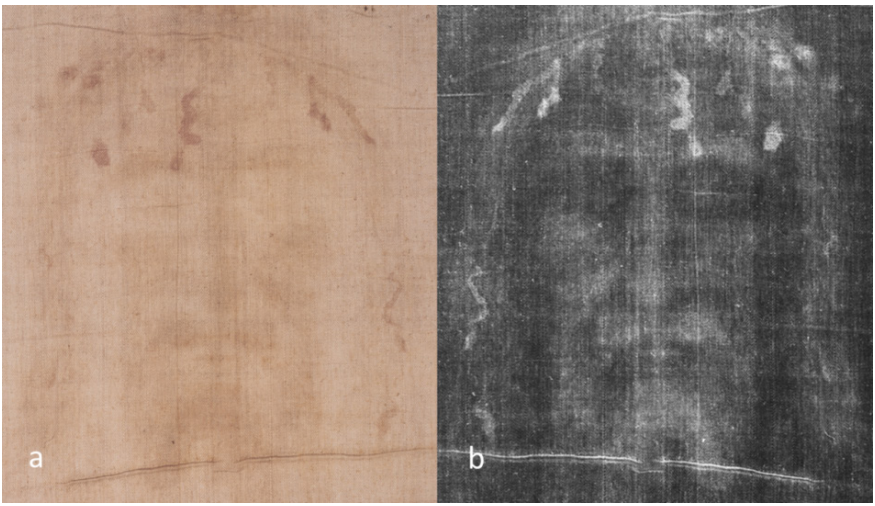


**Figure 1.** (**a**) original positive image of the TS face's region, extracted by a 2002 TS photograph realized by G. C. Durante; (**b**) absolute value of the logarithm of Fig. 1a, after the conversion in gray levels and specular inversion

sional information of the wrapped corpse, in terms of the yellowing of linen fibers.

The positive body image has been produced on the side where the linen sheet touched the corpse. Therefore, it is specular inverted and, consequently, it is common to invert left-right the negative image, with respect to the positive one. Figure 1b shows the absolute value of the logarithm of Figure 1a, after the conversion in gray levels and specular inversion. It is interesting to note as the absolute value of the logarithm of the intensities, shown in Figure 1b, depicts the right black and white contrast for a face (De Caro et al. 2019b) as if the photographed intensities followed a decreasing exponential law as a function of sheet-corpse distances. Of course, noise is amplified by the logarithmic displaying function, therefore the image shown in Fig. 1b needs some digital filtering to extract face information from artifacts and noise (De Caro and Giannini 2017).

We have already underlined that the spatial resolution of the anatomic details in the TS image is equal to 4.9±0.5 mm (Fanti and Basso 2009). The image shown in Fig. 1a consisted of 862 × 755 pixels, to which corresponds an area of about 26.3 × 23.0 $cm^2$. Thus, every pixel of Fig. 1a and 1b corresponds to a face's surface of about 0.3 × 0.3 $mm^2$, more than one order of magnitude finer than the TS body image's spatial resolution. As comparison, in the original image of G. C. Durante, at the pixels it corresponds a surface of about 0.05 × 0.05 $mm^2$, two orders of magnitude finer than the spatial resolution of the TS Man's image. These are 16-bit images.

## 3. TS body image details as a function of the radiation penetration depth in the cloth

Electromagnetic radiation penetrates textiles at different depths and interacts with their fibers as a function of photon energy and wavelength. To evidence the differences in terms of details of the body image, we compare the images obtained when the TS is illuminated by NIR, monochromatic visible light (blue, green, yellow and red) or by UV radiation.

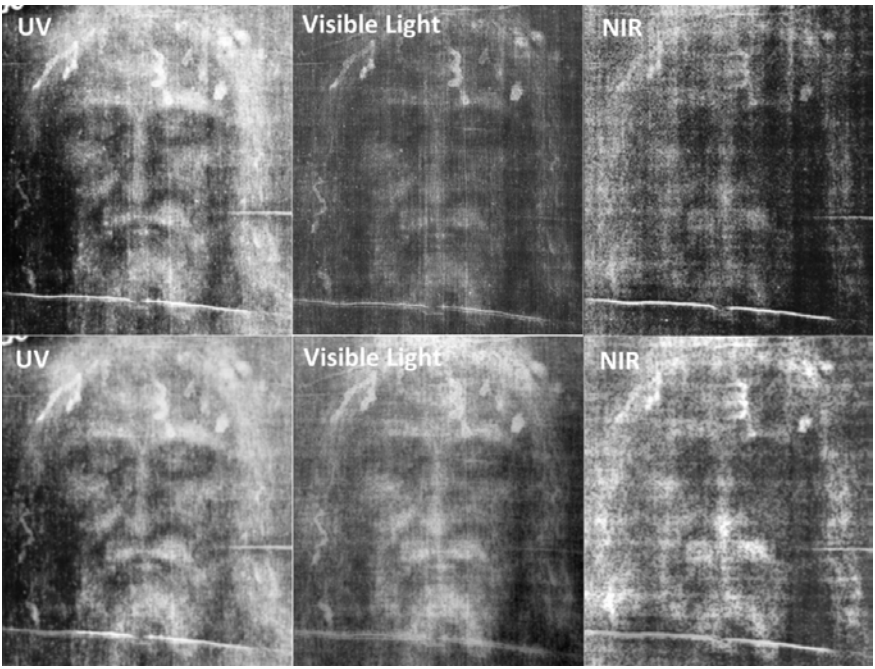


**Figure 2.** In the upper panels: absolute value of the logarithm of the TS face with specular inversion seen with UV, visible light and NIR radiations, after the conversion of images in gray levels. In the lower panels: same images after background stripes' correction, partial denoising and specular inversion

Figure 2 shows the UV and NIR acquisitions made by G. B. Judica Cordiglia in 1969 (Cordiglia 1976; 1988) compared with the face obtained by monochromatic visible light by W. Miller (Devan and Miller 1982), and visible light by G. Durante (Ghiberti 2002), after processing all the images with the same procedure described elsewhere (De Caro and Giannini 2017).[2]

To show how the TS face image's information changes as a function of the wavelength, and the corresponding penetration depth of radiation, Figure 2 shows the photograph taken by Durante (Ghiberti 2002) in vis-

[2] The UV and NIR photographs, used in this work, were bought by the second author directly from Judica Cordiglia, G. B. (2001). The photographs printed on paper have been digitized in 2398 x 3298 pixels by the second author using a scanner Epson Perfection 4490 Photo.

ible light, together with those illuminated with UV and NIR. We must observe that, as we will see in detail in the next section, UV photons are less penetrant than visible light photons which, in turn, are less penetrant than NIR ones. All the face's images shown in Fig. 2 were 600 × 526 pixels, to which corresponds an area of about 26.3 × 23.0 $cm^2$.

Thus, any pixel of six face's images of Fig. 2 corresponds to a face's surface of about 0.4 × 0.4 $mm^2$, always one order of magnitude finer the TS body image spatial resolution. In the original UV and NIR images of G. B. Judica Cordiglia at any pixel corresponds a face's surface of about 0.1 × 0.1 $mm^2$ and 0.05 × 0.05 $mm^2$, respectively. The images have an 8-bit depth. Therefore, the pixel resolution of the original images taken with the UV and NIR light is comparable to that of the Durante's TS images, taken with visible light. On the contrary, the bit depth of the UV and NIR images is half of that of the visible-light photos digitalized by G. C. Durante. However, also this is not a limiting factor because the spatial resolution of the body image is so worse, with respect to the pixel size, that the intensity variations, due to the contrast of different anatomical parts into the image, are slowly variable.

From the results shown in Fig. 2, we see that the eyelids appear more clearly highlighted by using the UV radiation; they are only partially visible with visible light and almost completely missing in the NIR image. This important characteristic of the TS face is further highlighted in Figure 3 where, in the upper panel, together with the UV and NIR results, we have inserted the acquisitions made by Miller (Devan and Miller 1982), who irradiated the cloth with wavelengths corresponding to blue, green and red light. Figure 3 shows the images obtained from the photographs after the conversion in gray levels, the usual inversion of the black and white contrast ($1 - I(x, y)$) and the specular inversion. The UV image has been acquired by using a mercury lamp. Therefore, the spectrum is known and the wavelength range [0.2–0.35] μm, containing the more intense Hg emission peaks, has been reported in the upper panel of Figure 3 in correspondence of the UV image. Instead, 0.9 μm is the limiting wavelength of the Kodak High Speed Infrared film HIE 135-36 used by Judica Cordiglia (Cordiglia 1976; 1988) to photograph the TS by using

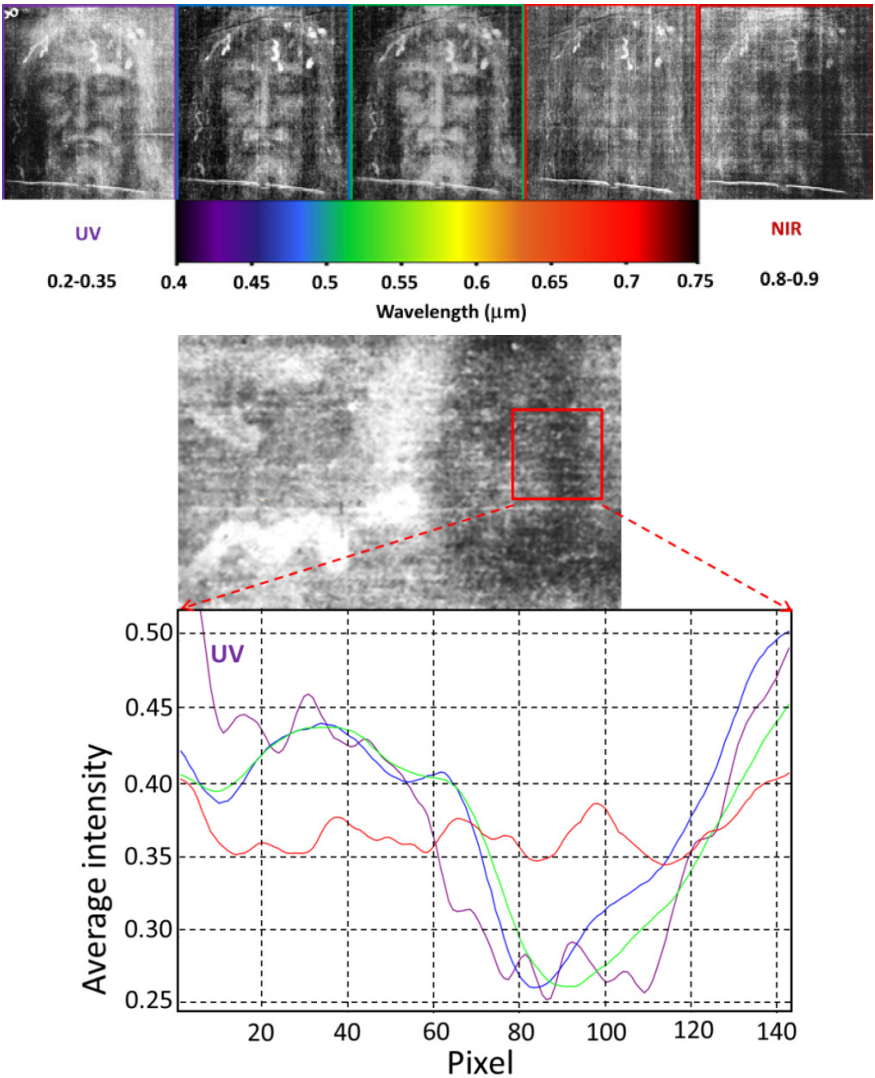


**Figure 3.** (**Upper panel**) From the left to the right: images of the TS face obtained by using radiation corresponding to the UV, blue, green, red and NIR wavelengths. UV and NIR photographs have been obtained by G. B. Judica Cordiglia; images with visible light have been obtained by the photographs of Miller. (**Lower panel**) Average intensity profiles in the red square region of the right eyelid, close to the three-shaped blood stain. UV indicates the profile of UV data, and red, blue and green curves are corresponding to the monochromatic visible light data shown in the upper panel

infrared radiation. Therefore, we put in correspondence of the NIR image (upper panel of Figure 3) the wavelength range of [0.8-0.9] μm. The wavelength values, used to realize the monochromatic photographs with visible light, shown in the upper panel of Figure 3, have been obtained by Miller by filtering the light: 0.45 μm for blue; 0.55 μm for green; 0.67 μm for red light. In the original monochromatic images acquired by Miller at any pixel corresponds a face's surface of about 0.1 × 0.1 $mm^2$. These images have an 8-bit depth. For the images shown in the upper panel of Fig. 3 at any pixel corresponds a face's surface of about 0.5 × 0.5 $mm^2$, about one order of magnitude finer than the TS body image's spatial resolution.

By analyzing the upper panel of Figure 3, it is evident that the anatomical details of the TS face become less detectable and definite as the wavelength increases, also in the range of the visible light. This finding has been evidenced, from a quantitatively point of view, in the lower panel of Figure 3. The plotted curves are the average intensity profiles in the red square region of the right eyelid, close to the three-shaped blood stain, for the TS image rotated counterclockwise of 90 degrees. In this way, the average profiles are almost perpendicular to the right eyelid's profile, thus showing the change of contrast at its end. UV indicates the profile of UV data (purple curve), and red, blue and green curves are corresponding to the monochromatic visible light data shown in the upper panel of Figure 3. These plots have been calculated by using the original images taken by Miller (Devan and Miller 1982), for which at any pixel corresponds a face's surface of about 0.1 × 0.1 $mm^2$. Therefore, the red square in the lower panel of Figure 3 spans an area of about 1.5 × 1.5 $cm^2$.

It is interesting to note that the red profile does not show any variation of average intensity at the end of the eyelid. The same behavior happens for the NIR image, not shown for clarity. Conversely, the UV (purple curve), blue and green profiles clearly show the end of the eyelid with a minimum of intensity. This minimum of intensity is characterized by a spatial width of about 0.6 cm for the UV image. Instead, it is about 0.4-0.5 cm wide for the blue and green images. For better understanding these important characteristics of the TS body image, in the next section we evaluate, theoretically, the attenuation lengths of electromagnetic radiation as it goes through the linen threads of the TS fabric.

## 4. Evaluation of the packing density of linen fibers in threads of the TS fabric

To estimate the packing density of linen fibers in a thread of the TS fabric, we need first to evaluate how dense is the packing of elementary linen fibers in the threads. Indeed, between the sections of the elementary linen fibers, of size 10-25 μm, there is always some void space. Visible electromagnetic radiation is attenuated by the 10-25 μm-sized linen fibers, but its absorption in few tens of μm of air can be neglected. Thus, the evaluation of the void space between the fibers is a pre-requisite for correctly estimating the attenuation of radiation of different wavelengths into the TS fabric.

The Turin Shroud is a woven 3/1 herringbone reversing twill fabric (Tyrer 1983). Figure 4a shows a section of the TS fabric, photographed by the second author. This section refers to a sample codified as F15001, and taken during the 1988 sampling, when the cloth was radiocarbon dated. The sample, therefore, comes from an area of the TS close to the corner of the 1988 sampling. The second author was allowed to analyze this sample, about 1 cm in size. The image resolution, in Fig. 4a, is of 1.35 μm, but the local variability of the TS thickness gives the following result.

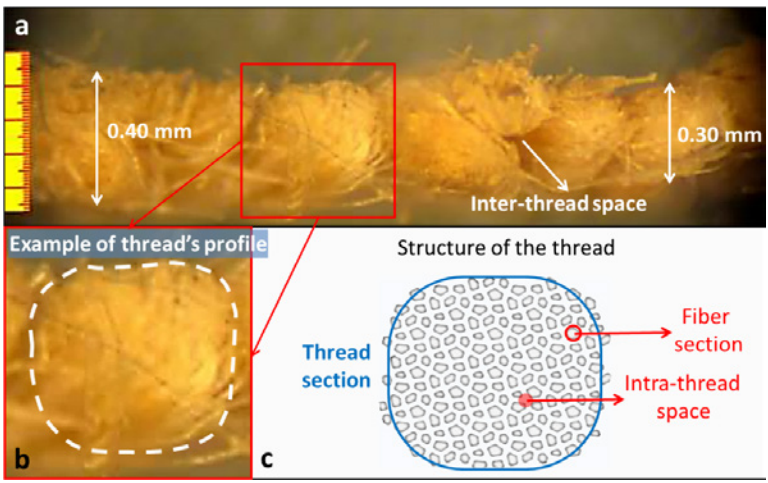


**Figure 4.** (**a**) Section of a sample of the TS fabric. (**b**) Example of a profile of a thread section. (**c**) Structure of the thread section with line fibers

The measured thickness, in this region of the cloth, is of 0.34±0.06 mm. Both the non-regular section and the variable thickness of the threads are evident. Figure 4b shows an example of the profile of a thread, where we can see that the sections of the threads are not perfectly circular. This characteristic is confirmed by a direct inspection of the TS fabric. This finding should be related to its compact weaving and manual manufacture. Figure 4c shows a schematic section of a linen thread which highlights the presence of inter-thread spaces, between the warp and weft threads, and intra-thread spaces, between the fibers of a single thread. Microscopically a thread is composed of 100–200 fibers. The thread packing density $\mu$ is defined as the ratio between the volume of the fibers divided by the volume of the thread (Køemenáková 2011). This parameter gives the degree of fiber compactness in a thread. Some numerical values of this parameter for the TS fabric can be derived from the technical report of G. Raes (Raes 1976), partially summarized by J. Tyrer (Tyrer 1983). The linen density reported in Table 1 has been obtained by averaging the values of Table 8 of (Amiri 2017).

For a fiber with circular section, the packing density $\mu$ can be calculated with the following formula (Køemenáková 2011):

$$\mu = \frac{T}{\frac{\pi}{4}\rho S^2} \cdot \tag{1}$$

where the size $S$ of the yarn is its diameter, ρ is the density of the material and $T$ is the thread fineness (see Table 1).

**Table 1. Textile parameters of the TS**

| | **Thread fineness T (linear density), measured in Tex (g/km)** | **Linen fiber density $\rho$ (Amiri 2017) (g/cm$^3$)** | **Thread size $S$ (μm)** |
|---|---|---|---|
| Weft | 53.6 | 1.5 | 250 |
| Warp | 16.3 | 1.5 | 140 |

Source: Tyrer 1983; Amiri 2017.

We have already underlined that the actual profiles of the TS threads' sections are not perfectly circular. For a generic profile Eq. (1) can be generalized with the following relation:

$$\mu = \frac{T}{a\rho S^2}. \qquad (2)$$

with the coefficient $a = \pi/4$ for a circular section, $a = 1$ for a square section, and intermediate values for real thread cross-sectional shapes like the TS one. For $\alpha = 0.9$, according to the values reported in Table 1, the packing density inside the threads is about 0.6.

However, thread packing density considers only the intra-thread space but not the inter-thread space, which is the void between different threads. Therefore, to evaluate the average packing density of the linen fibers in the whole TS fabric, the fabric density must be calculated (Adanur 1995; Vercelli 2010). To obtain the packing density of the fibers in the fabric, the density of the cloth has to be divided by the linen fibers' density (~1.5 g/cm$^3$), a ratio called packing factor and denoted $\boldsymbol{\mu_F}$. The thickness of the TS cloth, measured by J. P. Jackson with a micrometer, ranges from 0.32 to 0.39 mm (Jumper et al. 1984), confirmed by the second author (Fanti et al. 2020) who measured a mean thickness of 0.34 mm when studied the above-mentioned TS sample, named F15001. A section of this sample was measured both digitally, by means of the analysis of Figure 4a, and analogically, by using a centesimal caliber under a stereomicroscope, to avoid loading effects on the fabric produced by the feeler. Thus, from these measurements, a reliable average value of 0.35 mm (350 μm) can be considered. Because the average TS-cloth weight is 230±5 g/m$^2$ (Gilbert and Gilbert 1980**)** by using the average thickness 350 μm, the packing factor can be estimated as $\boldsymbol{\mu_F = 0.44 \pm 0.05}$. This packing factor is smaller than the estimated packing density $\mu$ because the former considers both inter- and intra-thread spaces. The ratio $\boldsymbol{\mu/\mu_F}$ gives an indirect measure of the thread compactness in the TS.

## 5. Different penetration depths of UV, visible and NIR radiation in the TS fabric

In this section we address the problem of calculating the attenuation of the radiation of different wavelengths in the TS cloth by using a Lambert-Beer Law approach:

$$\frac{I}{I_0} = exp\left[-z_{eff}/l(\lambda)\right] \tag{3}$$

where $I_0$ is the incident intensity of photons, $l(\lambda)$ is the attenuation length of photons having intensity $I$. This ratio is the inverse of the attenuation coefficient and depends on the wavelength. $Z_{eff}$, is the effective thickness of the fabric if all voids, intra-thread and inter-thread, were eliminated, reaching the maximum compaction of the linen fibers. Thus, $Z_{eff} = \mu_F \times z$, where $z$ is the actual fabric thickness.

Gilbert measured the reflectance of the TS in the framework of the STuRP research (Gilbert and Gilbert 1980). Some authors performed spectrophotometric measurements on a test linen fabric, manufactured according to the ancient technology (Di Lazzaro 2010). It has 15 threads/cm, the diameter of each thread is 300 μm, and the diameter of the single fiber ranges between 15 and 25 μm. The authors of (Di Lazzaro 2010) highlight the overlap of the measured absolute spectral reflectance values of the test linen with Gilbert's data.

Moreover, the spectral absorption $A(\lambda)$ of the test linen was estimated by the measured absolute spectral reflectance and transmittance values. Thanks to the overlapping between the reflectance measurements obtained on the test linen fabric with those obtained on the TS, we can assume similar microscopic characteristics, in terms of fiber packing density and packing factor, between the two fabrics.

The spectral absorption $A(\lambda)$ can be related to Eq. (3) through the following relation:

$$exp\left[-z_{eff}/l(\lambda)\right] = 1 - A(\lambda), \tag{4}$$

where $Z_{eff} \cong 150$ μm is the effective thickness of the linen fibers in the fabric, eliminating both inter-thread and intra-thread voids. Eq. (4) allows to estimate the attenuation length of light, as a function of the wavelength, in a linen fabric like the TS. The absorption measurements in (Di Lazzaro 2010) were performed up to 0.6 μm wavelength values. The absolute spectral reflectance measurements in (Gilbert and Gilbert 1980) on the TS were performed up to 0.75 μm, confirming a linear dependence as a function of the wavelength also in the range 0.6–0.75 μm.

Indeed, absorption of light shows a linear dependence as a function of the wavelength up to the NIR values of about 1.0 μm. The values measured in (Di Lazzaro 2010) have been summarized in Table 2, together with the linearly extrapolated values up to 0.9 μm, which is the limiting wavelength of the Kodak High Speed Infrared film HIE 135-36 used by Judica Cordiglia (Cordiglia 1976;1988) to photograph the TS at the infrared radiation. From Table 2 and Eq. (4) it is possible to estimate $l(\lambda)$ at different wavelengths. The results are shown in Table 3. The estimated variability of the attenuation length is due to the indetermination of the quantities from which it depends. The trend of the spectral absorption $A(\lambda)$ is almost linear and slowly variable with the wavelength.

**Table 2. Estimated spectral absorption A($\lambda$) in a linen fabric having features like the TS. The data for wavelengths larger than 600 are extrapolated**

| $\lambda$ [nm] | 200 | 250 | 300 | 350 | 400 | 450 | 500 | 550 | 600 | 650 | 700 | 800 | 900 |
|---|---|---|---|---|---|---|---|---|---|---|---|---|---|
| A($\lambda$) | 0.91 | 0.86 | 0.81 | 0.75 | 0.69 | 0.63 | 0.58 | 0.54 | 0.50 | 0.46 | 0.42 | 0.34 | 0.26 |

Therefore, although actual $A(\lambda)$ values, measured on the TS, are not available, nevertheless, the estimated values reported in Table 2 can be used to evaluate the attenuation lengths reported in Table 3, since the images analyzed in this paper were taken at very wide wavelength intervals from one another, separated by about 100-200 nm. In other words, the poor knowledge of the TS $A(\lambda)$ function can be tolerated because, to evaluate the attenuation lengths reported in Table 3, the spectral absorption values are required at coarse wavelength steps of about 100–200 nm.

A complex physical/chemical process, not fully clarified by studies, impressed the body image of a human corpse on the linen cloth. Moreover, all body image information is concentrated in the topmost superficial elementary fibers of the threads (Fanti et al. 2010). During the STuRP campaign in 1978, R. Rogers directly analyzed, by means of a magnification lens, the maximum depth of the body image in correspondence of the image of nose, and found that the image was so superficial that its thickness was not more than the topmost three fibers of a colored thread, i.e., about 70 μm (Schwalbe and Rogers 1982). Moreover, on these superficial fibers the color is localized on the surface of the TS fibers, in a layer of about 0.2 μm thick, named the primary cell wall (Fanti et al. 2010).

**Table 3. Estimated attenuation length $l(\lambda)$ of photons in a linen fabric like the TS**

| Range of $\lambda$ [nm] | $l(\lambda)$ [μm] |
|---|---|
| 200–350 (UV) | 75–95 |
| 450 (Blue) | 130–170 |
| 550 (Green) | 170–220 |
| 700 (Red) | 240–310 |
| 750–900 (NIR) | 340–440 |

These findings have been summarized in Figure 5.

In Fig. 5a a schematic TS cloth cross-section is represented together with the different attenuation lengths of UV, visible light and NIR radiations. The width of the colored rectangles, associated to the different $l(\lambda)$, are due to the indeterminations on the calculated attenuation length values. Fig. 5b shows the attenuation of the intensity of radiation with different wavelengths inside the TS fabric, predicted by Eq. (4) and the values reported in Table 3. The attenuation lengths – distances at which the intensity is reduced to 1/e of the initial value – are given by the intersection of the colored curves with the horizontal black line. Note that the UV value of attenuation length is close to the yellowing superficial layer thickness, corresponding to the depth of about three fibers inside the fabric. Thus, from Fig. 5 the UV light is confined to the more super-

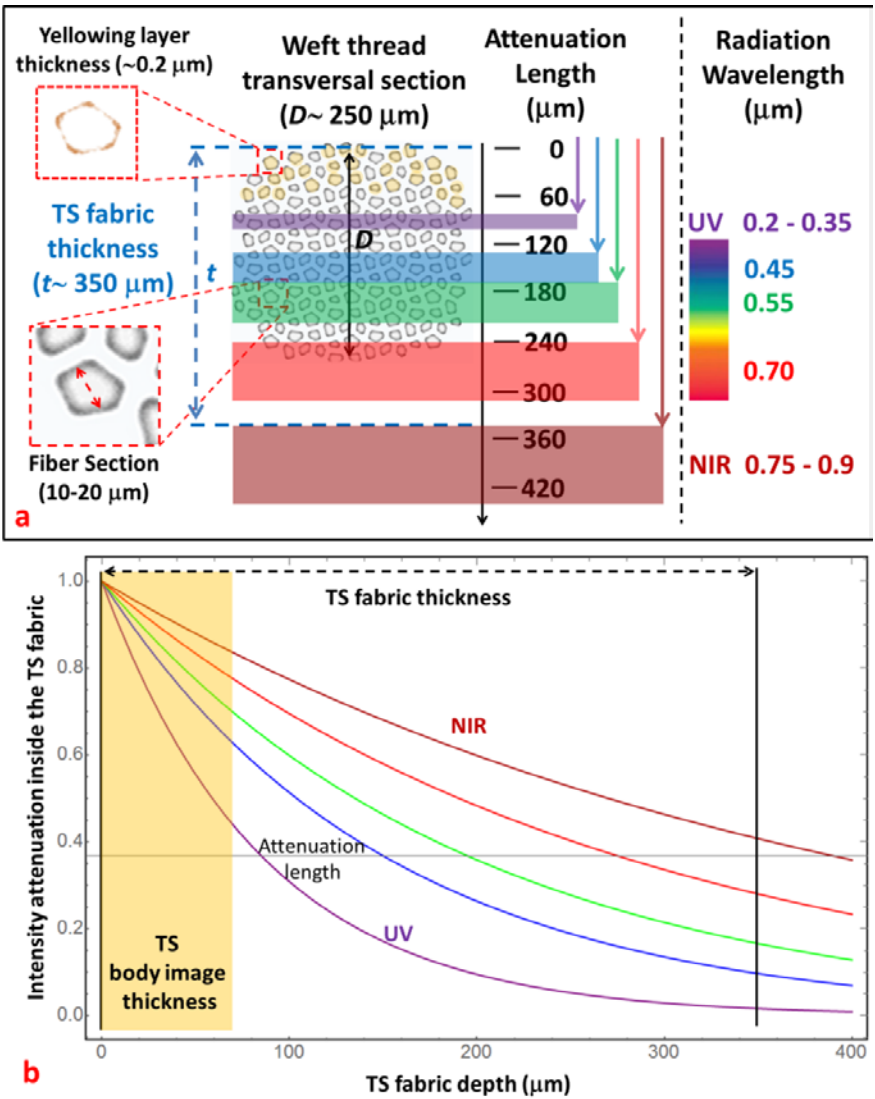


**Figure 5.** (**a**) Schematic TS cloth cross-section with the different attenuation lengths of UV, visible light and NIR radiations inside the fabric. The width of the colored rectangles is due to the indeterminations of the calculated attenuation length values. (**b**) Attenuation of intensity of radiation with different wavelength inside the TS fabric. The attenuation lengths are given by the intersection of colored curves with the horizontal black line

ficial part of the TS fabric, where the body image is embedded. Instead, visible light photons travel more in depth, and the reflected light contains information relative to the body image together with that of many uncolored linen fibers. Photons in the NIR, instead, can go through the whole TS fabric. It should be also noted that the reflected light intensity is attenuated along its optical path twice: the first, to reach the inner fibers; then to return to the entrance fabric surface. Therefore, the body images obtained by using UV and blue light show well-defined anatomic details, because these are embedded in the topmost superficial linen fibers. The more penetrant the radiation the smaller the contribution to the whole body-image of the more superficial fibers, highlighted in yellow in Fig. 5.

These results explain, from a quantitative point of view, what has been qualitatively shown in Fig. 3, where red light and NIR give poor defined anatomic details of the face of the TS Man. A comparison between the photographs with blue and red light, both produced by W. Miller supposedly by using the same digitalizing procedure, evidences that the body images present different contrast levels. The red image of face shows a lower contrast than the blue and UV images: the information regarding eyes, cheeks and mouth almost disappears on the image obtained with red light, while the image obtained with blue light shows much better the anatomic features in those areas.

This fact may also support a new hypothesis: the image intensity does not depend only on the areal density of colored fibers in a thread (Jumper et al. 1984), but also on their volumetric density which depends on the total number of colored fibers reached by the light in the *whole* fabric depth. In other words, the depth of the color layer could be variable along the TS surface: where the image is more intense (tip of the nose) the depth is about 70 μm (about three colored fibers in the thread), as directly detected by Ray Rogers during the STuRP campaign); but it could become thinner (two or one colored fibers) where the TS image is less intense. The confirmation of this hypothesis would require a dedicated study, a more accurate direct microscopical inspection of the TS image in different regions of the body image characterized by different contrast's values.

## 6. The body image at the exit surface of the TS

When looking at the TS in 2002 after the removal of the backing cloth sewed by the Chambery nuns in 1534, G. Ghiberti (2002) noted the presence of a very feeble new body image on the backside, in correspondence of the hair. G. Fanti and R. Maggiolo (2014), after proper image processing, noted a whole image of the face and, perhaps, hands on the backside of the TS, but P. Di Lazzaro and coworkers (Di Lazzaro et al. 2013) imputed this face to a pareidolia effect, but this hypothesis was confuted (Fanti et al. 2014).

After results on the light transmission through the TS fabric, here discussed, we will here reconsider the problem of the double superficiality of the TS body image. Indeed, the results previously discussed could imply that, with visible light, the body image on the front TS surface could be not so intense and deep to contribute to the reflected intensity when the fabric is illuminated on the backside. To exclude the possibility to see the superficial body image when the TS is observed on the backside, we can impose ideal conditions, unphysical in real materials, but useful to estimate an upper limit to the maximum possible intensity that can travel through the whole fabric thickness, acquire some body image information and, finally, reemerge from the entrance surface. To this task, we can assume the following ideal conditions which would give the maximum possible transfer of body image information from one side to the other, for a backside illumination: 1) the shortest possible path inside the fabric (path perpendicular to the back-side surface); 2) the body image information, contained in the first 70 μm of thickness, on the TS front side, can be carried out by the radiation, exiting from the entrance surface, the TS backside. This ideal situation has been schematically in the inset of Fig. 6. The plotted curves in Fig. 6 show the attenuation of the different visible light spectral components (blue, green and red) inside the TS fabric, under the above assumptions. With this regard, we note that, one could readily use the values of Table 3 when plotting Fig. 6, by calculating the fraction of the transmitted intensity at the depth z, for light in the visible range.

The inset shown in Fig. 6 reports, graphically, where the intensity corresponding to the different spectral components would reach 10% of the initial values, according to Eqs (3–4) and the above assumptions. Even assuming the above ideal conditions, which would facilitate the transmission of the image through the TS thickness, only about 5% of the whole incident visible light intensity on the TS backside would reemerge from the same side, after having reached the TS front-side. In fact, only the most superficial layer, of thickness of about 70 μm (about three linen fibers), contains the body image information of the TS Man.

Indeed, the fractions of transmitted intensities of red, green and blue light, at the end of the round-trip optical path inside the cloth, are given by the final values of the plotted curves in Fig. 6: about 0.10, 0.04 and

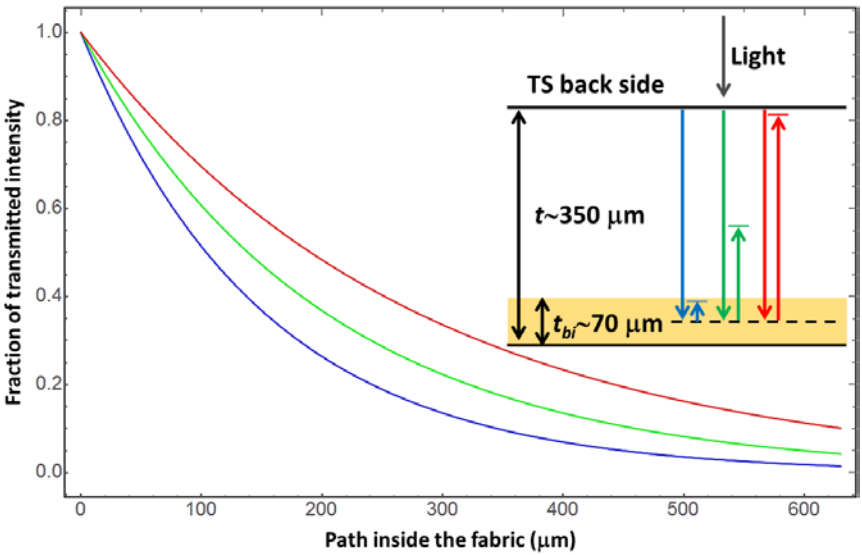


**Figure 6:** Attenuation of the different visible light spectral components (blue, green and red) inside the TS fabric assuming back side illumination and the following unphysical ideal conditions: 1) shortest path inside the fabric; 2) the body image information, contained in the first 70 μm of thickness (*t*bi), on the TS front side, can be carried out by the radiation, exiting from the entrance surface, the TS backside. The inset shows where the intensity corresponding to the different spectral components would reach 10% of the initial value

0.01, respectively. Therefore, the average value for visible light is about 0.05. However, as already underlined, not all the above assumptions are satisfied in real cases. In fact, light impinges on cloth with an angle different from 90°. Consequently, the path of light inside the cloth will not be perpendicular to the TS surfaces and, therefore, the total path inside the cloth will be quite longer than $2 \times t$, where $t$ is the TS thickness. Moreover, it is impossible to have: *i*) total reflection of light on the TS exit side for radiation impinging on the TS backside, after the light goes through the whole fabric; *ii*) straight optical propagation of light.

Indeed, the microscopic structure of a linen thread is particularly inhomogeneous, from the optical point of view, because regions composed of cellulose (linen fibers), with refractive index values about 1.5, alternate with air regions (interspaces between fibers) with a refractive index 1. In a non-homogeneous microstructure, the light is scattered in any direction and does not propagate by reflection, since the continuous change of the refractive index from 1 to 1.5 causes multiple refraction and scattering, making the medium opaque (De Caro et al. 2018). In addition, we know that, in opaque media, total reflection at the surface of separation between the media and the air, for radiation impinging perpendicularly on it, is not possible. Consequently, the estimate that 5% of the whole incident intensity on the TS back-side would reemerge from the same side, after having reached the TS front-side, can be considered a largely overestimated upper bound. Actual values are at least one order of magnitude less than 5%. Therefore, we can conclude that less than 1% of the body image information, embedded in the top-layer of the TS front-side, can contribute to the reflected image of the backside when this surface of the cloth is photographed with visible light, as made by G. Durante in 2002 (Ghiberti 2002).

This result can be readily confirmed by searching to see a superficial stain on a linen fabric with threads of thickness of about 0.35 mm, from the other side of the fabric, back illuminating the stain. Therefore, we performed the following experimental test to further demonstrate that there is no correlation between the two images of TS face, that of the front and that of the backside. A cross was painted with a charcoal on

a TS-like linen fabric (leaned on a white plane, that is the worst case) and it was photographed on both sides of the sheet (see Figure 7a).

Fig. 7b shows a photograph of the backside, specular reversed left right, to be directly compared to the image of the front-side (Fig. 7a). The red arrows indicate a fold of the fabric that can be taken as a reference feature to verify the absence of any image of the charcoal cross on the backside of the fabric. Only the four black dots realized by a spirit color goes through the whole thickness of the fabric, because the liquid penetrates deep into the threads. Conversely, the superficial black charcoal cross is not visible on the other side. With this regard it should be stressed that the black color of the charcoal cross with respect to the background color of the linen fabric is characterized by an elevate contrast in terms of gray levels. Conversely, on the TS the image contrast is obtained by the difference between two yellow shades: the first corresponding to the body region; the second one corresponding to the background with no image. Therefore, for the TS the maximum image contrast is surely much less than that one obtainable by a "black" charcoal cross on a linen fabric's background. Also, this empirical evidence, indirectly, indicates that any probable body image of the TS Man, visible on the backside of the fabric, could be related to the superficial front-side top-layer.

After the above considerations, to better visualize what is visible on the TS backside, we have applied the same digital analysis approach, previously described for the results shown in Fig. 2 (De Caro et al. 2017), to

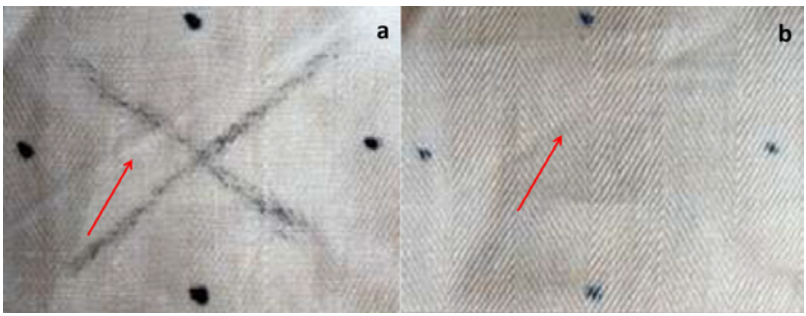


**Figure 7.** (**a**) photo of a cross-painted by means of a charcoal on a TS-like linen fabric; (**b**) photo of the back side, specular reversed left-right, to be directly comparable with the image of the front-side (Fig. 7a). The red arrows indicated a fold of the fabric

the photograph acquired in visible light by G. C. Durante (Ghiberti 2002) on the backside of the cloth. We display the obtained results in Figure 8.

It is shown how the logarithm of the body image on the back of the TS, seen with visible light, in correspondence of the face region, presents

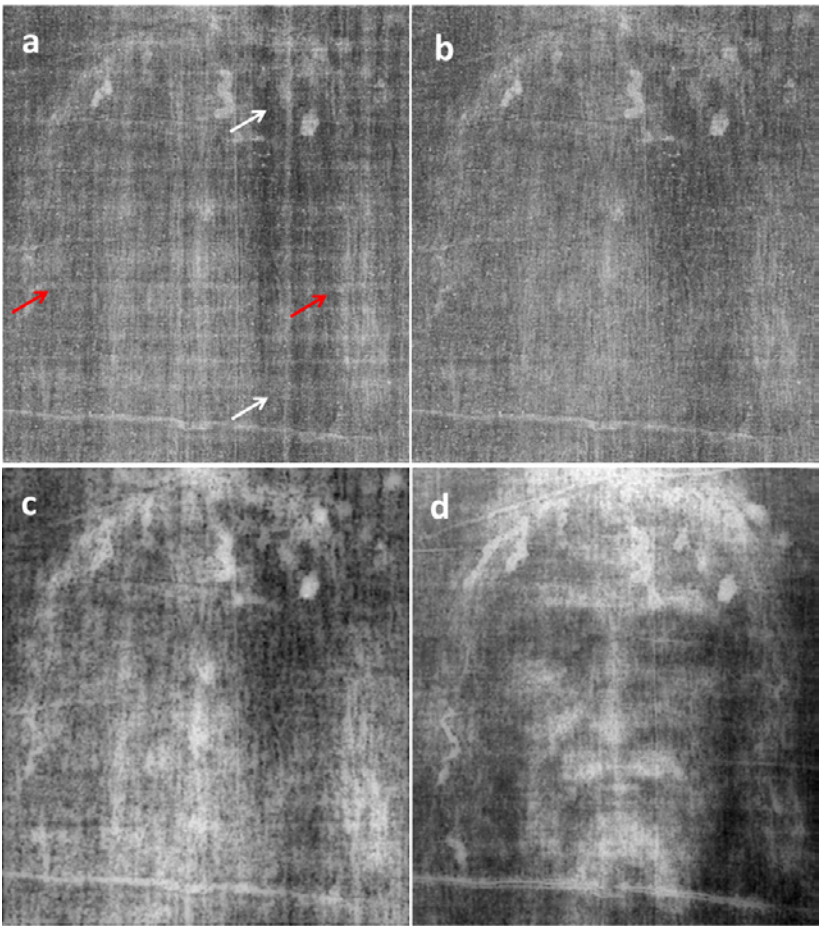


**Figure 8.** (**a**) Logarithm of the body image on the back of the TS, seen with visible light, in correspondence with the region of the face. The white arrows indicate an example of vertical stripes; the red arrows indicate an example of horizontal stripes. (**b**) Digital removal of the stripes. (**c**) Image of the backside of the TS obtained after denoising. (**d**) Equivalent image of Fig. 8c for the body image on the front side of the TS, in direct contact with the wrapped body, in correspondence of the region of the face

many artifacts principally due to the low contrast of the image. For example, the white arrows indicate some vertical stripes; the red arrows some horizontal stripes (Fig. 8a). Fig. 8b shows the result obtained after digital removal of these stripes by using the approach described elsewhere (De Caro et al. 2017). Fig. 8c shows the final image, obtained also after denoising, and it is compared with the corresponding image for the body image on the front side of the TS (Fig. 8d). We notice how, after the digital processing, a semblance of face is also visible on the back of the TS (Fig. 8c), although it has a lower spatial resolution; it seems to be laterally more deformed and presents much less defined anatomic details. Nevertheless, a body image of the face seems visible also on the back of the cloth, i.e., on the surface which was not in contact with the corpse.

In Figure 9 we show the integrated scans in the area of the red rectangle, in correspondence of the tip of the nose for the TS front side image (left) and backside (right). The plots have been normalized with respect to the maximum value, reached in correspondence of the tip of the nose, which is surely a point of contact of the corpse with the cloth. The integrated scans shown in Fig. 9 seem to indicate that also the backside image could contain quantitative information of the distances of some anatomic parts from the cloth surface.

Therefore, the quantitative results shown in Fig. 9 and the resemblances between Fig. 8c and 8d are so many that make possible to exclude that we are dealing with a pareidolia effect, as supposed in (Di Lazzaro et al. 2013). In particular, in addition to the image of hair glimpsed by G. Ghiberti in 2002, in Fig. 8 also eyebrows, beard and mouth appear on the post-processed image, confirming the conclusions discussed in (Fanti 2003; Fanti et al. 2014). This means that the fabric presents a superficial image on one side, no image in the middle, and another superficial image on the opposite side.

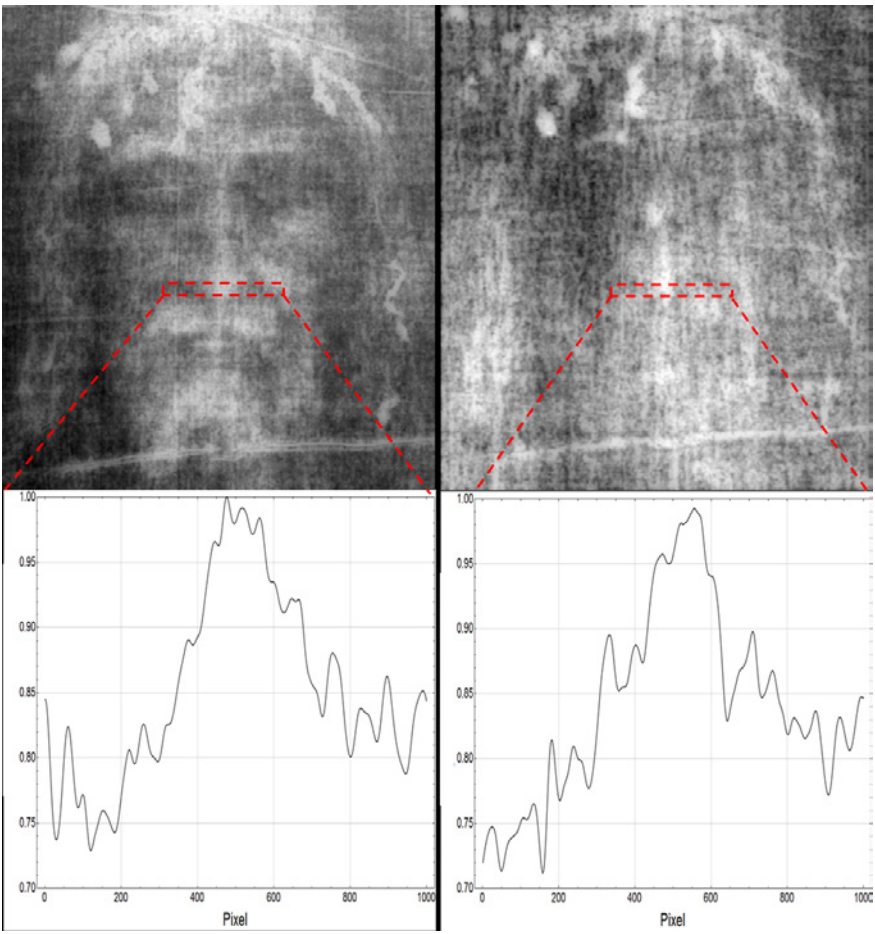


**Figure 9.** Integrated scans in the red rectangle in correspondence of the tip of the nose for the TS front side image (left) and backside (right)

## 7. Discussion and conclusions

We have shown that, by changing the wavelength, from UV tor NIR, anatomical details of the TS face become increasingly less detectable and definite. The more the radiation penetrates into the fabric the fewer anatomical details are visible. These results confirm the extreme superficiality of the body image on the TS cloth, equivalent to the depth correspond-

ing to about three linen fibers. Moreover, a detailed quantitative analysis of the attenuation of light during propagation in a linen fabric, together with some experimental tests performed on a linen fabric characterized by the same thickness and weave of the TS, support the hypothesis that the depth, to which the TS body image arrives into the fabric, could also be a function of the distance of the various anatomical parts from the cloth surface. In other words, it cannot be excluded that the TS body image depth could be locally variable. Consequently, the intensity of the TS body image could depend not only on the areal density of yellowed linen fibers, but also on their volumetric density, up to a maximum depth of about 70 μm.

Furthermore, our digital analysis seems to indicate that even on the backside of the TS –the surface not in contact with the human body – another body image is visible, even if more evanescent. Putting this result together with the analysis about the attenuation lengths of visible light, we should conclude that this body information could not be due to superficial yellowed fibers of the front side of the TS. Therefore, we conclude that there is a double superficiality of the TS body image, with no information in between the two cloth surfaces.

Evidently, all the above results must be related to the TS body-image formation process. The corona discharge hypothesis (Fanti 2009) could explain this double superficiality from a microscopic point of view, but it seems to be less efficient to predict other characteristics of the TS body image. Therefore, we should probably consider a more complex imaging phenomenon not only linked to an electric source like that proposed by (Fanti 2023; Fanti and Siefker 2024) in connection with the Holy Fire of Jerusalem coupled with the urea exudate from the corpse. In any case, even if in laboratory, with a peculiar source of energy, all the chemical/physical properties of the TS body image would be fully experimentally obtained, nevertheless, since a corpse of a dead man cannot give off radiant energy in the right wavelength range, to activate the processes of oxidation, dehydration and conjugation of the polysaccharides composing the body-image linen fibers, we should conclude that the TS body image will remain a mystery for science.

Conversely, according to faith, the human body of a living Man should emit energy, during his resurrection from death, assuming a transition to a different state of matter, characterizing a new immortal corpse, as explicitly revealed that it will happen for each of us (cf. 1 Cor 15,35-58) and witnessed by early Christians already happened for Jesus Christ and his mother. We already know that *only* about 4% of the whole universe is constituted by ordinary matter, constituting our corpses, and in all the world many astronomers, cosmologists, particle physicists are searching for new states of matter, that certainly exist but that have not been yet discovered. Also, the Holy Fire, visible in Holy Sepulcher of Jerusalem every year (Fanti 2023; Fanti et al. 2024) just in the period of the Orthodox Easter, could be considered a not-ordinary form of energy that, in principle, could give useful insights for a deeper understanding of the TS body-image's process of formation. For these reasons, we could think to the TS as a two-thousand-old relic which witness to the humanity, just in the age of science, the reasonableness of the faith in the resurrection.

We know that the TS body image is characterized by an almost vertical projection on the cloth, implying a directional flux of intense energy, from the body towards the cloth, at the origin of the body image. But a corpse cannot emit intense and directional energy, suitable to imprint into a linen cloth a body image as it is observed on the TS. Thermal energy can be emitted by a corpse, until the equilibrium with the environment is reached, but it is neither intense nor directional.

Moreover, from the analysis of the cadaveric data of a body and the proposed presence of face life signs (Hontanilla 2022), a new hypothesis has been raised: the TS body-image's features could correspond to a living person, moving inside the cloth, *after* his coming back from death to life. An alternative hypothesis, which is more convincing for us, is that while the TS was wrapping the corpse of a tortured and dead man – for the authors, Jesus of Nazareth – an inexplicable phenomenon from a scientific point of view occurred: an intense energy impressed the image of his body *right at the moment* He returned back to life. This energy, which would have impressed the body image on the TS, should be related precisely to the transition from the death to life, from a corpse in a possible

state of rigor mortis (Bevilacqua et al. 2018) to a living body. According to (Hontanilla, 2022) signs of live are present in the face image impressed on the TS. Under this hypothesis, it is also possible that this energy could correspond directly to Christ alive, after his death. However, in the former case, this energy should be related to a change of the state of matter of the risen body, in the transition from death to life, from a corruptible to an incorruptible state (cf. 1 Cor 15,42), characterized also by new physical properties, such as the possibility of inter-penetrability with the ordinary matter, as witnessed by the Gospels (cf. Jh 20,19), thus leading to the possibility for the risen body to go through the burial cloth. Indeed, the TS image is double-sided, just due to the assumed directional emission of this energy during the Resurrection; it is not single-sided. Therefore, the TS image can be considered a snapshot witnessing the transition from death to life (resurrection).

In any case, whatever is the hypothesis we assume for schematizing resurrection in terms of biological, medical, space-time and energy-matter concepts, since it is not reproducible in laboratory, it goes beyond the actual possibility of analysis of science and, consequently, we should limit our investigations on what we see and measure on the TS, i.e. the body image with its chemical and physical properties, which has been the main topic of this work. Nevertheless, it is important to conclude highlighting the most important point of all the discussion: we do not know any chemical/physical process that could generate an intense and directional energy, either from a corpse or from a living man, made of ordinary matter, able to impress the image of his body on his burial cloth, with all the microscopical and macroscopical properties that studies have evidenced on the TS which, until now, has not yet *fully* reproduced in any laboratory and experiment, notwithstanding the technology and knowledge today available. For this reason, the body image of TS remains without any satisfactory explanation for science. Therefore, it can be also considered as indirect evidence that in a tomb of Jerusalem, about 2000 years ago, a phenomenon occurred that goes beyond the knowledge of modern science: the Resurrection of a corpse, that of Jesus Christ, as the Christian faith teaches us to believe.

**Conflicts of Interest:** The authors declare no conflict of interest and no funding.

## References

Adanur, Sabit. 1995. *Wellington Sears Handbook of Industrial textiles*, CRC Press: 626.

Adler, Alan. 2014. *The Orphaned Manuscript: A Gathering of Publications on the Shroud of Turin*. Cantalupa (TO), Italy: Effatà.

Amiri, Ali, Zach Triplett, Augusto Moreira, Noa Brezinka, Mercedes Alcock, and Chad A. Ulven. 2017. "Standard density measurement method development for flax fiber." *Industrial Crops and Products* 96: 196–202. DOI: https://doi.org/10.1016/j.indcrop.2016.11.060.

Antonacci, Mark. 2016. *Test The Shroud: At the Atomic and Molecular Levels*. USA: Forefront Publishing Company.

Balossino, Nello. 2003. "Sul retro della Sindone non vi è impronta: osservazione diretta ed elaborazioni informatiche." *Sindon* 19: 57–69.

Barbet, Pierre. 2014. *A Doctor at Calvary: the passion of our Lord Jesus Christ as described by a surgeon*. Allegro Editions.

Bevilacqua, Matteo et al., 2018. "Rigor Mortis and News obtained by the Body's Scientific Reconstruction of the Turin Shroud Man." *Peertechz J Forensic Sci Technol* 4: 001–008. DOI: http://dx.doi.org/10.17352/pjfst.000010.

Casabianca, Tristan, et al. 2019. *Radiocarbon dating of the Turin Shroud: New evidence from raw data*, *Archeometry* 61: 1223–31. DOI: https://doi.org/10.1111/arcm.12467.

Damon, Paul E., et al. 1989. "Radiocarbon dating of the Shroud of Turin." *Nature* 337: 611–15. DOI: https://doi.org/10.1038/337611a0.

De Caro, Liberato, and Cinzia Giannini. 2017. "Turin Shroud hands' region analysis reveals the scrotum and a part of the right thumb." *Journal of Cultural Heritage* 24: 140–6. DOI: https://doi.org/10.1016/j.culher.2016.10.015.

De Caro, Liberato, Emilio Matricciani, and Giulio Fanti. 2018. "Imaging analysis and digital restoration of the Holy Face of Manoppello – Part I." *Heritage* 1: 19. DOI: https://doi.org/10.3390/heritage1020019.

De Caro, Liberato, Cinzia Giannini, Rocco Lassandro, Francesco Scattarella, Teresa Sibillano, Emilio Matricciani, and Giulio Fanti. 2019a "X-ray dating of ancient linen fabrics." *Heritage* 2: 2763–83. DOI: https://doi.org/10.3390/heritage2040171.

De Caro, Liberato, Emilio Matricciani, and Giulio Fanti. 2019b. "A comparison between the Face of the Veil of Manoppello and the Face of the Shroud of Turin." *Heritage* 2: 339–55. DOI: https://doi.org/10.3390/heritage2010023.

De Caro, Liberato, Teresa Sibillano, Rocco Lassandro, Cinzia Giannini, and Giulio Fanti. 2022a. "X–ray Dating of a Turin Shroud's Linen Sample." *Heritage* 5: 860–70. DOI: https://doi.org/10.3390/heritage5020047.

De Caro, Liberato. 2020. Il volto sVelato, Isola del Liri (Fr), Italy: Centro Editoriale Valtortiano.

De Caro, Liberato, César Barta, Giulio Fanti, Emilio Matricciani, Teresa Sibillano, and Cinzia Giannini. 2022b. "Long-Term Temperature Effects on the Natural Linen Aging of the Turin Shroud." *Information* 13: 458. DOI: https://doi.org/10.3390/info13100458.

De Caro, Liberato. 2024. *Sindone – Un mistero millenario*, Verona, Italy: Fede & Cultura.

De Caro, Liberato, and Emilio Matricciani. 2024. *Imprints of Jesus of Nazareth: The Veil and the Shroud*, Newcastle upon Tyne, UK: Cambridge Scholar Publishing.

Devan, Don. 1982. "Quantitative photography of the Shroud of Turin" In *IEEE Proc. Int. Conf. on Cybernetics and Society*, October 1982. https://www.shroud.com/pdfs/Quantitative%20Photography%20Devan%20Miller%201982%20OCRsm.pdf.

Di Lazzaro, Paolo, Daniele Murra, Antonino Santoni, Giulio Fanti, Enrico Nichelatti, and Giuseppe Baldacchini. 2010. "Deep Ultraviolet Radiation Simulates the Turin Shroud Image." *Journal of Imaging Science and Technology* 54: 040302-040306.

Di Lazzaro, Paolo, Daniele Murra, and Barrie Schwortz. 2013. "Pattern recognition after image processing of low-contrast images, the case of the Shroud of Turin." *Pattern Recognition* 46: 1964–70. DOI: https://doi.org/10.1016/j.patcog.2012.12.010.

Fanti, Giulio. 2003. "Commenti sulla doppia superficialità dell'immagine frontale dell'Uomo della Sindone di Torino." *Sindon* 19: 83–8.

Fanti, Giulio, and Roberto Maggiolo. 2004. "The double superficiality of the frontal image of the Turin Shroud," *J. Opt. A: Pure Appl. Opt*. 6: 491–503. DOI: 10.1088/1464-4258/6/6/001.

Fanti, Giulio. 2009. "Body image formation hypotheses based on corona discharge: discussion." In *Proceedings of the Shroud Science Group International Conference the Shroud of Turin: Perspectives on a Multifaceted Enigma*, Columbus, OH, USA, 14–17 August 2008. Padova, Italy: Libreria Progetto.

Fanti, Giulio, and Roberto Basso. 2009. "MTF Resolution of Images Obtained without an Acquisition System." In *Proceedings of the Shroud Science Group International Conference the Shroud of Turin: Perspectives on a Multifaceted Enigma*, Columbus, OH, USA, 14–17 August 2008. Padova, Italy: Libreria Progetto.

Fanti, Giulio, et al. 2010. "Microscopic and Macroscopic characteristics of the Shroud of Turin Image Superficiality." *Journal of Imaging Science and Technology* 54: 040201–040208.

Fanti, Giulio. 2011. "Hypotheses regarding the formation of the body image on the Turin Shroud. A critical compendium." *J. of Imaging Sci. Technol.* 55: 060507. DOI: https://doi.org/10.2352/J.ImagingSci.Technol.2011.55.6.060507.

Fanti, Giulio, and Roberto Maggiolo. 2014. "About the second image of face detected on the Turin Shroud." In *Int. Conference on the "Shroud of Turin: The Controversial Intersection of Faith and Science."* St. Louis, Missouri, USA, October 9-12, 2014. https://www.shroud.com/pdfs/stlfanti1.pdf.

Fanti. Giulio, and Pierandrea Malfi. 2015a. *The Shroud of Turin – First century After Christ!* Singapore: Pan Stanford Publishing.

Fanti Giulio, Pierandrea Malfi, and Fabio Crosilla. 2015b. "Mechanical and optochemical dating of Turin Shroud." *MATEC Web of Conferences* 36: 01001. DOI: https://doi.org/10.1051/matecconf/20153601001.

Fanti, Giulio. 2018. "Why is the Turin Shroud Authentic?" *Glob J Arch & Anthropol.* 7: 555707. DOI: 10.19080/GJAA.2018.07.555707.

Fanti, Giulio. 2023. "Holy Fire and Body Image of the Holy Shroud: Divine Photography Hypothesis." *World Scientific News WSN* 176: 104–20.

Fanti, Giulio, and Robert Siefker. 2024. *The Holy Fire and the Divine Photography – The Image of the Holy Shroud of Christ,* Jenny Stanford Series on Christian Relics and Phenomena, Vol. 6, Jenny Stanford Pub.

Ghiberti, Giuseppe. 2002. *2002 Shroud images*. Torino, Italy: ODPF Ed.

Gilbert, Roger, and Marion M. Gilbert. 1980. "Ultraviolet-visible reflectance and fluorescence spectra of the Shroud of Turin." *Appl. Opt*. 19: 1930–36. DOI: https://doi.org/10.1364/AO.19.001930.

Hontanilla, Bernardo. 2022. "The Man of the Shroud of Turin: Is He Dead or Alive?" *Scientia et Fides* 10(1): 91–114. DOI: https://doi.org/10.12775/SetF.2022.005.

Jackson, John. 2017. *The Shroud of Turin: A Critical Summary of Observations, Data and Hypotheses*, USA: Catholic Shoppe. http://www.shroudofturin.com/Resources/CRTSUM.pdf.

Jackson, John P. 1998. "Does the Shroud of Turin Show Us the Resurrection?" Madrid, España: Escuela Biblica Ed., pp. 217–40.

Judica Cordiglia, Giovanni Battista. 1976. “Come si è proceduto alla ripresa fotografica della SS. Sindone in occasione della ricognizione privata del 18 giugno 1969.” *Rivista Diocesana Torinese* (Supplemento): 93–101.

Judica Cordiglia Giovanni Battista 1988. “Ricerche ed indagini di laboratorio sulle fotografie eseguite nel 1969.” In *Proc. IV Nat. Congr. Of Studies on the Turin Shroud*, edited by Cinisello Balsamo, 132–141, Milano, Italy: Ed. Paoline.

Jumper, Eric, Alan A. Adler, John P. Jackson, Samuel F. Pellicori, John H. Heller, and James R. Druzik. 1984. “A comprehensive examination of the various stains and images on the Shroud of Turin.” *Advances in Chemistry* 3: 447–76. DOI: 10.1021/ba-1984-0205.ch022.

Køemenáková, Dana, Rajesh Mishra, Jiøí Militký and Jaroslav Šesták. 2011. *Selected topics of textile and material science*. Pilsen: Publishing House of WBU.

Moran, Kevin, and Giulio Fanti. 2002. “Does the Shroud body image show any physical evidence of Resurrection?” IV Symposium Scientifique International du CIELT, Paris, France, https://www.sindone.info/MORAN1.PDF.

Raes, Gilbert. 1976. “Rapport d’analyse.” In *La S. Sindone. Ricerche e studi della commissione di esperti nominata dall’Arcivescovo di Torino*. Turin, Italy: Supplemento Rivista diocesana torinese.

Riani, Marco, Anthony C. Atkinson, Giulio Fanti, and Fabio Crosilla. 2013. “Regression analysis with partially labeled regressors: carbon dating of the Shroud of Turin.” *Statistics and Computing* 23: 551–61. DOI: https://doi.org/10.1007/s11222-012-9329-5.

Rogers, Raymond. 2005. “Studies on the radiocarbon sample from the Shroud of Turin.” *Thermochimica Acta* 425: 189–94. DOI: 10.1016/j.tca.2004.09.029.

Schwalbe Larry A., and R. N. Rogers. 1982. “Physics and chemistry of the Shroud of Turin.” a summary of the 1978 investigation.” *Analytica Chimica Acta* 135: 3–49. DOI: https://doi.org/10.1016/S0003-2670(01)85263-6.

Tyrer, John. 1983. “Looking at the Turin Shroud as a textile.” *Shroud Spectrum International* 6: 35–45.

Vercelli, Piero. 2010. *La Sindone nella sua struttura tessile*. Cantalupa (TO), Italy: Effatà.

Wilson, Ian. 2011. *The Shroud. Fresh light on the 2000-year-old Mystery*. London, UK: Bantam.